Search for scalar top quarks in the acoplanar charm jets and missing transverse energy final state in $p\bar{p}$ collisions at $\sqrt{s} = 1.96$ TeV

V.M. Abazov[36], B. Abbott[75], M. Abolins[65], B.S. Acharya[29], M. Adams[51], T. Adams[49], E. Aguilo[6], S.H. Ahn[31], M. Ahsan[59], G.D. Alexeev[36], G. Alkhazov[40], A. Alton[64,a], G. Alverson[63], G.A. Alves[2], M. Anastasoaie[35], L.S. Ancu[35], T. Andeen[53], S. Anderson[45], B. Andrieu[17], M.S. Anzelc[53], M. Aoki[50], Y. Arnoud[14], M. Arov[60], M. Arthaud[18], A. Askew[49], B. Åsman[41], A.C.S. Assis Jesus[3], O. Atramentov[49], C. Avila[8], C. Ay[24], F. Badaud[13], A. Baden[61], L. Bagby[50], B. Baldin[50], D.V. Bandurin[59], P. Banerjee[29], S. Banerjee[29], E. Barberis[63], A.-F. Barfuss[15], P. Bargassa[80], P. Baringer[58], J. Barreto[2], J.F. Bartlett[50], U. Bassler[18], D. Bauer[43], S. Beale[6], A. Bean[58], M. Begalli[3], M. Begel[73], C. Belanger-Champagne[41], L. Bellantoni[50], A. Bellavance[50], J.A. Benitez[65], S.B. Beri[27], G. Bernardi[17], R. Bernhard[23], I. Bertram[42], M. Besançon[18], R. Beuselinck[43], V.A. Bezzubov[39], P.C. Bhat[50], V. Bhatnagar[27], C. Biscarat[20], G. Blazey[52], F. Blekman[43], S. Blessing[49], D. Bloch[19], K. Bloom[67], A. Boehnlein[50], D. Boline[62], T.A. Bolton[59], G. Borissov[42], T. Bose[77], A. Brandt[78], R. Brock[65], G. Brooijmans[70], A. Bross[50], D. Brown[81], N.J. Buchanan[49], D. Buchholz[53], M. Buehler[81], V. Buescher[22], V. Bunichev[38], S. Burdin[42,b], S. Burke[45], T.H. Burnett[82], C.P. Buszello[43], J.M. Butler[62], P. Calfayan[25], S. Calvet[16], J. Cammin[71], W. Carvalho[3], B.C.K. Casey[50], H. Castilla-Valdez[33], S. Chakrabarti[18], D. Chakraborty[52], K. Chan[6], K.M. Chan[55], A. Chandra[48], F. Charles[19,‡], E. Cheu[45], F. Chevallier[14], D.K. Cho[62], S. Choi[32], B. Choudhary[28], L. Christofek[77], T. Christoudias[43], S. Cihangir[50], D. Claes[67], Y. Coadou[6], M. Cooke[80], W.E. Cooper[50], M. Corcoran[80], F. Couderc[18], M.-C. Cousinou[15], S. Crépé-Renaudin[14], D. Cutts[77], M. Ćwiok[30], H. da Motta[2], A. Das[45], G. Davies[43], K. De[78], S.J. de Jong[35], E. De La Cruz-Burelo[64], C. De Oliveira Martins[3], J.D. Degenhardt[64], F. Déliot[18], M. Demarteau[50], R. Demina[71], D. Denisov[50], S.P. Denisov[39], S. Desai[50], H.T. Diehl[50], M. Diesburg[50], A. Dominguez[67], H. Dong[72], L.V. Dudko[38], L. Duflot[16], S.R. Dugad[29], D. Duggan[49], A. Duperrin[15], J. Dyer[65], A. Dyshkant[52], M. Eads[67], D. Edmunds[65], J. Ellison[48], V.D. Elvira[50], Y. Enari[77], S. Eno[61], P. Ermolov[38], H. Evans[54], A. Evdokimov[73], V.N. Evdokimov[39], A.V. Ferapontov[59], T. Ferbel[71], F. Fiedler[24], F. Filthaut[35], W. Fisher[50], H.E. Fisk[50], M. Fortner[52], H. Fox[42], S. Fu[50], S. Fuess[50], T. Gadfort[70], C.F. Galea[35], E. Gallas[50], C. Garcia[71], A. Garcia-Bellido[82], V. Gavrilov[37], P. Gay[13], W. Geist[19], D. Gelé[19], C.E. Gerber[51], Y. Gershtein[49], D. Gillberg[6], G. Ginther[71], N. Gollub[41], B. Gómez[8], A. Goussiou[82], P.D. Grannis[72], H. Greenlee[50], Z.D. Greenwood[60], E.M. Gregores[4], G. Grenier[20], Ph. Gris[13], J.-F. Grivaz[16], A. Grohsjean[25], S. Grünendahl[50], M.W. Grünewald[30], F. Guo[72], J. Guo[72], G. Gutierrez[50], P. Gutierrez[75], A. Haas[70], N.J. Hadley[61], P. Haefner[25], S. Hagopian[49], J. Haley[68], I. Hall[65], R.E. Hall[47], L. Han[7], K. Harder[44], A. Harel[71], R. Harrington[63], J.M. Hauptman[57], R. Hauser[65], J. Hays[43], T. Hebbeker[21], D. Hedin[52], J.G. Hegeman[34], J.M. Heinmiller[51], A.P. Heinson[48], U. Heintz[62], C. Hensel[58], K. Herner[72], G. Hesketh[63], M.D. Hildreth[55], R. Hirosky[81], J.D. Hobbs[72], B. Hoeneisen[12], H. Hoeth[26], M. Hohlfeld[22], S.J. Hong[31], S. Hossain[75], P. Houben[34], Y. Hu[72], Z. Hubacek[10], V. Hynek[9], I. Iashvili[69], R. Illingworth[50], A.S. Ito[50], S. Jabeen[62], M. Jaffré[16], S. Jain[75], K. Jakobs[23], C. Jarvis[61], R. Jesik[43], K. Johns[45], C. Johnson[70], M. Johnson[50], A. Jonckheere[50], P. Jonsson[43], A. Juste[50], E. Kajfasz[15], A.M. Kalinin[36], J.M. Kalk[60], S. Kappler[21], D. Karmanov[38], P.A. Kasper[50], I. Katsanos[70], D. Kau[49], V. Kaushik[78], R. Kehoe[79], S. Kermiche[15], N. Khalatyan[50], A. Khanov[76], A. Kharchilava[69], Y.M. Kharzheev[36], D. Khatidze[70], T.J. Kim[31], M.H. Kirby[53], M. Kirsch[21], B. Klima[50], J.M. Kohli[27], J.-P. Konrath[23], V.M. Korablev[39], A.V. Kozelov[39], J. Kraus[65], D. Krop[54], T. Kuhl[24], A. Kumar[69], A. Kupco[11], T. Kurča[20], J. Kvita[9], F. Lacroix[13], D. Lam[55], S. Lammers[70], G. Landsberg[77], P. Lebrun[20], W.M. Lee[50], A. Leflat[38], J. Lellouch[17], J. Leveque[45], J. Li[78], L. Li[48], Q.Z. Li[50], S.M. Lietti[5], J.G.R. Lima[52], D. Lincoln[50], J. Linnemann[65], V.V. Lipaev[39], R. Lipton[50], Y. Liu[7], Z. Liu[6], A. Lobodenko[40], M. Lokajicek[11], P. Love[42], H.J. Lubatti[82], R. Luna[3], A.L. Lyon[50], A.K.A. Maciel[2], D. Mackin[80], R.J. Madaras[46], P. Mättig[26], C. Magass[21], A. Magerkurth[64], P.K. Mal[82], H.B. Malbouisson[3], S. Malik[67], V.L. Malyshev[36], H.S. Mao[50], Y. Maravin[59], B. Martin[14], R. McCarthy[72], A. Melnitchouk[66], L. Mendoza[8], P.G. Mercadante[5], M. Merkin[38], K.W. Merritt[50], A. Meyer[21], J. Meyer[22,d], T. Millet[20], J. Mitrevski[70], J. Molina[3], R.K. Mommsen[44], N.K. Mondal[29], R.W. Moore[6], T. Moulik[58], G.S. Muanza[20], M. Mulders[50], M. Mulhearn[70], O. Mundal[22], L. Mundim[3], E. Nagy[15], M. Naimuddin[50], M. Narain[77], N.A. Naumann[35], H.A. Neal[64], J.P. Negret[8], P. Neustroev[40], H. Nilsen[23], H. Nogima[3], S.F. Novaes[5], T. Nunnemann[25], V. O'Dell[50], D.C. O'Neil[6], G. Obrant[40], C. Ochando[16], D. Onoprienko[59], N. Oshima[50], N. Osman[43], J. Osta[55], R. Otec[10], G.J. Otero y Garzón[50], M. Owen[44], P. Padley[80], M. Pangilinan[77], N. Parashar[56], S.-J. Park[71], S.K. Park[31],

J. Parsons[70], R. Partridge[77], N. Parua[54], A. Patwa[73], G. Pawloski[80], B. Penning[23], M. Perfilov[38], K. Peters[44], Y. Peters[26], P. Pétroff[16], M. Petteni[43], R. Piegaia[1], J. Piper[65], M.-A. Pleier[22], P.L.M. Podesta-Lerma[33,c], V.M. Podstavkov[50], Y. Pogorelov[55], M.-E. Pol[2], P. Polozov[37], B.G. Pope[65], A.V. Popov[39], C. Potter[6], W.L. Prado da Silva[3], H.B. Prosper[49], S. Protopopescu[73], J. Qian[64], A. Quadt[22,d], B. Quinn[66], A. Rakitine[42], M.S. Rangel[2], K. Ranjan[28], P.N. Ratoff[42], P. Renkel[79], S. Reucroft[63], P. Rich[44], J. Rieger[54], M. Rijssenbeek[72], I. Ripp-Baudot[19], F. Rizatdinova[76], S. Robinson[43], R.F. Rodrigues[3], M. Rominsky[75], C. Royon[18], P. Rubinov[50], R. Ruchti[55], G. Safronov[37], G. Sajot[14], A. Sánchez-Hernández[33], M.P. Sanders[17], A. Santoro[3], G. Savage[50], L. Sawyer[60], T. Scanlon[43], D. Schaile[25], R.D. Schamberger[72], Y. Scheglov[40], H. Schellman[53], T. Schliephake[26], C. Schwanenberger[44], A. Schwartzman[68], R. Schwienhorst[65], J. Sekaric[49], H. Severini[75], E. Shabalina[51], M. Shamim[59], V. Shary[18], A.A. Shchukin[39], R.K. Shivpuri[28], V. Siccardi[19], V. Simak[10], V. Sirotenko[50], P. Skubic[75], P. Slattery[71], D. Smirnov[55], G.R. Snow[67], J. Snow[74], S. Snyder[73], S. Söldner-Rembold[44], L. Sonnenschein[17], A. Sopczak[42], M. Sosebee[78], K. Soustruznik[9], B. Spurlock[78], J. Stark[14], J. Steele[60], V. Stolin[37], D.A. Stoyanova[39], J. Strandberg[64], S. Strandberg[41], M.A. Strang[69], E. Strauss[72], M. Strauss[75], R. Ströhmer[25], D. Strom[53], L. Stutte[50], S. Sumowidagdo[49], P. Svoisky[55], A. Sznajder[3], P. Tamburello[45], A. Tanasijczuk[1], W. Taylor[6], J. Temple[45], B. Tiller[25], F. Tissandier[13], M. Titov[18], V.V. Tokmenin[36], T. Toole[61], I. Torchiani[23], T. Trefzger[24], D. Tsybychev[72], B. Tuchming[18], C. Tully[68], P.M. Tuts[70], R. Unalan[65], L. Uvarov[40], S. Uvarov[40], S. Uzunyan[52], B. Vachon[6], P.J. van den Berg[34], R. Van Kooten[54], W.M. van Leeuwen[34], N. Varelas[51], E.W. Varnes[45], I.A. Vasilyev[39], M. Vaupel[26], P. Verdier[20], L.S. Vertogradov[36], M. Verzocchi[50], F. Villeneuve-Seguier[43], P. Vint[43], P. Vokac[10], E. Von Toerne[59], M. Voutilainen[68,e], R. Wagner[68], H.D. Wahl[49], L. Wang[61], M.H.L.S. Wang[50], J. Warchol[55], G. Watts[82], M. Wayne[55], G. Weber[24], M. Weber[50], L. Welty-Rieger[54], A. Wenger[23,f], N. Wermes[22], M. Wetstein[61], A. White[78], D. Wicke[26], G.W. Wilson[58], S.J. Wimpenny[48], M. Wobisch[60], D.R. Wood[63], T.R. Wyatt[44], Y. Xie[77], S. Yacoob[53], R. Yamada[50], M. Yan[61], T. Yasuda[50], Y.A. Yatsunenko[36], K. Yip[73], H.D. Yoo[77], S.W. Youn[53], J. Yu[78], A. Zatserklyaniy[52], C. Zeitnitz[26], T. Zhao[82], B. Zhou[64], J. Zhu[72], M. Zielinski[71], D. Zieminska[54], A. Zieminski[54,‡], L. Zivkovic[70], V. Zutshi[52], and E.G. Zverev[38]

(The DØ Collaboration)

[1]*Universidad de Buenos Aires, Buenos Aires, Argentina*
[2]*LAFEX, Centro Brasileiro de Pesquisas Físicas, Rio de Janeiro, Brazil*
[3]*Universidade do Estado do Rio de Janeiro, Rio de Janeiro, Brazil*
[4]*Universidade Federal do ABC, Santo André, Brazil*
[5]*Instituto de Física Teórica, Universidade Estadual Paulista, São Paulo, Brazil*
[6]*University of Alberta, Edmonton, Alberta, Canada,*
Simon Fraser University, Burnaby, British Columbia,
Canada, York University, Toronto, Ontario, Canada,
and McGill University, Montreal, Quebec, Canada
[7]*University of Science and Technology of China, Hefei, People's Republic of China*
[8]*Universidad de los Andes, Bogotá, Colombia*
[9]*Center for Particle Physics, Charles University, Prague, Czech Republic*
[10]*Czech Technical University, Prague, Czech Republic*
[11]*Center for Particle Physics, Institute of Physics,*
Academy of Sciences of the Czech Republic, Prague, Czech Republic
[12]*Universidad San Francisco de Quito, Quito, Ecuador*
[13]*LPC, Univ Blaise Pascal, CNRS/IN2P3, Clermont, France*
[14]*LPSC, Université Joseph Fourier Grenoble 1, CNRS/IN2P3,*
Institut National Polytechnique de Grenoble, France
[15]*CPPM, IN2P3/CNRS, Université de la Méditerranée, Marseille, France*
[16]*LAL, Univ Paris-Sud, IN2P3/CNRS, Orsay, France*
[17]*LPNHE, IN2P3/CNRS, Universités Paris VI and VII, Paris, France*
[18]*DAPNIA/Service de Physique des Particules, CEA, Saclay, France*
[19]*IPHC, Université Louis Pasteur et Université de Haute Alsace, CNRS/IN2P3, Strasbourg, France*
[20]*IPNL, Université Lyon 1, CNRS/IN2P3, Villeurbanne, France and Université de Lyon, Lyon, France*
[21]*III. Physikalisches Institut A, RWTH Aachen, Aachen, Germany*
[22]*Physikalisches Institut, Universität Bonn, Bonn, Germany*
[23]*Physikalisches Institut, Universität Freiburg, Freiburg, Germany*
[24]*Institut für Physik, Universität Mainz, Mainz, Germany*
[25]*Ludwig-Maximilians-Universität München, München, Germany*
[26]*Fachbereich Physik, University of Wuppertal, Wuppertal, Germany*
[27]*Panjab University, Chandigarh, India*

[28] *Delhi University, Delhi, India*

[29] *Tata Institute of Fundamental Research, Mumbai, India*

[30] *University College Dublin, Dublin, Ireland*

[31] *Korea Detector Laboratory, Korea University, Seoul, Korea*

[32] *SungKyunKwan University, Suwon, Korea*

[33] *CINVESTAV, Mexico City, Mexico*

[34] *FOM-Institute NIKHEF and University of Amsterdam/NIKHEF, Amsterdam, The Netherlands*

[35] *Radboud University Nijmegen/NIKHEF, Nijmegen, The Netherlands*

[36] *Joint Institute for Nuclear Research, Dubna, Russia*

[37] *Institute for Theoretical and Experimental Physics, Moscow, Russia*

[38] *Moscow State University, Moscow, Russia*

[39] *Institute for High Energy Physics, Protvino, Russia*

[40] *Petersburg Nuclear Physics Institute, St. Petersburg, Russia*

[41] *Lund University, Lund, Sweden, Royal Institute of Technology and Stockholm University,*
Stockholm, Sweden, and Uppsala University, Uppsala, Sweden

[42] *Lancaster University, Lancaster, United Kingdom*

[43] *Imperial College, London, United Kingdom*

[44] *University of Manchester, Manchester, United Kingdom*

[45] *University of Arizona, Tucson, Arizona 85721, USA*

[46] *Lawrence Berkeley National Laboratory and University of California, Berkeley, California 94720, USA*

[47] *California State University, Fresno, California 93740, USA*

[48] *University of California, Riverside, California 92521, USA*

[49] *Florida State University, Tallahassee, Florida 32306, USA*

[50] *Fermi National Accelerator Laboratory, Batavia, Illinois 60510, USA*

[51] *University of Illinois at Chicago, Chicago, Illinois 60607, USA*

[52] *Northern Illinois University, DeKalb, Illinois 60115, USA*

[53] *Northwestern University, Evanston, Illinois 60208, USA*

[54] *Indiana University, Bloomington, Indiana 47405, USA*

[55] *University of Notre Dame, Notre Dame, Indiana 46556, USA*

[56] *Purdue University Calumet, Hammond, Indiana 46323, USA*

[57] *Iowa State University, Ames, Iowa 50011, USA*

[58] *University of Kansas, Lawrence, Kansas 66045, USA*

[59] *Kansas State University, Manhattan, Kansas 66506, USA*

[60] *Louisiana Tech University, Ruston, Louisiana 71272, USA*

[61] *University of Maryland, College Park, Maryland 20742, USA*

[62] *Boston University, Boston, Massachusetts 02215, USA*

[63] *Northeastern University, Boston, Massachusetts 02115, USA*

[64] *University of Michigan, Ann Arbor, Michigan 48109, USA*

[65] *Michigan State University, East Lansing, Michigan 48824, USA*

[66] *University of Mississippi, University, Mississippi 38677, USA*

[67] *University of Nebraska, Lincoln, Nebraska 68588, USA*

[68] *Princeton University, Princeton, New Jersey 08544, USA*

[69] *State University of New York, Buffalo, New York 14260, USA*

[70] *Columbia University, New York, New York 10027, USA*

[71] *University of Rochester, Rochester, New York 14627, USA*

[72] *State University of New York, Stony Brook, New York 11794, USA*

[73] *Brookhaven National Laboratory, Upton, New York 11973, USA*

[74] *Langston University, Langston, Oklahoma 73050, USA*

[75] *University of Oklahoma, Norman, Oklahoma 73019, USA*

[76] *Oklahoma State University, Stillwater, Oklahoma 74078, USA*

[77] *Brown University, Providence, Rhode Island 02912, USA*

[78] *University of Texas, Arlington, Texas 76019, USA*

[79] *Southern Methodist University, Dallas, Texas 75275, USA*

[80] *Rice University, Houston, Texas 77005, USA*

[81] *University of Virginia, Charlottesville, Virginia 22901, USA and*

[82] *University of Washington, Seattle, Washington 98195, USA*

(Dated: March 14, 2008)

We present a search for the pair production of scalar top quarks, $\tilde{t}$, using 995 pb^{-1} of data collected in $p\bar{p}$ collisions with the D0 detector at the Fermilab Tevatron Collider at $\sqrt{s} = 1.96$ TeV. Both scalar top quarks are assumed to decay into a charm quark and a neutralino ($\tilde{\chi}_1^0$), where $\tilde{\chi}_1^0$ is the lightest supersymmetric particle. This leads to a final state with two acoplanar charm jets and missing transverse energy. We find the yield of such events to be consistent with the standard model expectation, and exclude sets of $\tilde{t}$ and $\tilde{\chi}_1^0$ masses at the 95% C.L. that substantially extend

the domain excluded by previous searches.

Supersymmetry (SUSY) may provide a solution to the hierarchy problem if the SUSY particles have masses less than 1 TeV, strongly motivating the searches for supersymmetric objects at the Fermilab Tevatron Collider. SUSY predicts the existence of partners with identical quantum numbers to all standard model (SM) particles except for spin. There exist two spin zero SUSY partners of the top quark corresponding to the latter's left and right handed states. Several arguments exist in favor of a light scalar top quark ($\tilde{t}$). The $\tilde{t}$ mass $m_{\tilde{t}}$ receives negative contributions proportional to the top quark Yukawa coupling in the renormalization group equations. This makes the $\tilde{t}$ weak eigenstates lighter than other squarks [1]. Mixing between the left and right handed superpartners of the top quark, being proportional to the top quark mass m_t, leads to a large mass splitting between the two physical eigenstates. This makes one of the $\tilde{t}$ considerably lighter than the other. Additionally, a light $\tilde{t}$ that strongly couples to the Higgs boson could also generate a large enough CP violating phase to explain the mechanism for electroweak baryogenesis [2].

In R-parity conserving models [3], the lightest supersymmetric particle (LSP) is stable, and cosmological constraints indicate that it should be neutral and colorless [4]. In the following we assume conservation of R-parity and take $\tilde{\chi}_1^0$, the lightest of four SUSY particles that result from the mixing between the SUSY partners of the SM neutral gauge and Higgs bosons, to be the LSP.

In the search reported in this Letter, we consider the range $m_{\tilde{t}} < m_b + m_{\tilde{\chi}_1^+}$ and $m_{\tilde{t}} < m_W + m_b + m_{\tilde{\chi}_1^0}$, where m_b is the b quark mass, $m_{\tilde{\chi}_1^0}$ is the $\tilde{\chi}_1^0$ mass and $m_{\tilde{\chi}_1^+}$ is the $\tilde{\chi}_1^+$ mass, with $\tilde{\chi}_1^+$ being the lighter of two mass eigenstates resulting from the mixing of the SUSY partners of charged gauge and Higgs bosons. The dominant $\tilde{t}$ decay mode in this model is the flavor changing process $\tilde{t} \to c\tilde{\chi}_1^0$ and is assumed to occur with 100% branching fraction. The $\tilde{t} \to t\tilde{\chi}_1^0$ decay is kinematically forbidden over the $\tilde{t}$ mass range accessible in this search, and the tree level four-body decays $\tilde{t} \to b f \bar{f}' \tilde{\chi}_1^0$ can be neglected [5].

In $p\bar{p}$ collisions, $\tilde{t}$ pairs are produced via quark-antiquark annihilation and gluon fusion. The $\tilde{t}$ pair production cross section ($\sigma_{\tilde{t}\bar{\tilde{t}}}$) primarily depends on $m_{\tilde{t}}$, and a weak dependence on other SUSY parameters affects only the higher-order corrections. At $\sqrt{s} = 1.96$ TeV which is the centre-of-mass energy available at the Fermilab Tevatron collider, $\sigma_{\tilde{t}\bar{\tilde{t}}}$ at next-to-leading-order (NLO), calculated with PROSPINO [6], ranges from 15 pb to 1 pb for $100 \leq m_{\tilde{t}} \leq 160$ GeV. These cross sections are calculated using CTEQ6.1M parton distribution functions (PDFs) [7] and equal renormalization and factorization

scales $\mu_{\rm rf} = m_{\tilde{t}}$. A theoretical uncertainty of $\approx 20\%$ is estimated due to scale and PDF choices. The $\tilde{t}\bar{\tilde{t}}$ event topology consists of two acoplanar charm jets and missing transverse energy ($\not{E}_T$) from the neutralinos that escape detection. Searches for $\tilde{t}$ pair production in the jets plus missing transverse energy mode have been reported by collaborations working at the CERN LEP collider [8], and the CDF [9, 10] and D0 [11, 12] collaborations. The highest excluded mass to date is $m_{\tilde{t}} < 134$ GeV (95% C.L.) for $m_{\tilde{\chi}_1^0} = 48$ GeV [12].

The $\tilde{t}$ search is performed in the data collected with the D0 detector during Run IIa of the Tevatron and corresponds to an integrated luminosity of 995 ± 61 pb^{-1} [13]. A detailed description of the D0 detector can be found in [14]. The central tracking system consists of a silicon microstrip tracker and a fiber tracker, both located within a 2 T superconducting solenoidal magnet. A liquid-argon and uranium calorimeter covers pseudorapidity $|\eta| \lesssim 4.2$, where $\eta = -\ln[\tan(\theta/2)]$, and θ is the polar angle with respect to the proton beam direction. An outer muon system, covering $|\eta| < 2$, consists of layers of tracking detectors and scintillation counters on both sides of 1.8 T iron toroids.

The data sample collected from April 2003 to February 2006 with the jets+$\not{E}_T$ triggers was analyzed for the $\tilde{t}$ search. The trigger conditions require the $\not{H}_T$ and its separation from all jets to be greater than 30 GeV and 25°, respectively, where $\not{H}_T$ is the transverse energy computed only from jets. Jets are reconstructed using an iterative midpoint cone algorithm with radius $\mathcal{R}_{\rm cone} = 0.5$ [15]. The data set is reduced to a sample of 1.5 million events by requiring at least two jets with $p_T > 15$ GeV and $\not{E}_T > 40$ GeV.

Signal samples are simulated using PYTHIA 6.323 [16] for $m_{\tilde{t}}$ ranging from 95 GeV to 165 GeV and $\tilde{\chi}_1^0$ masses from 45 GeV to 90 GeV. The largest expected backgrounds for this search are W and Z bosons produced in association with jets, denoted as V+jets. The V+jets and $t\bar{t}$ processes are simulated using ALPGEN 2.05 [17] interfaced with PYTHIA for the generation of initial and final state radiation and hadronization. The background samples for single top quark and diboson production are simulated using COMPHEP [18] and PYTHIA, respectively. The PDF set CTEQ6L1 is used for both signal and background samples, and all generated events are subjected to full GEANT-based [19] simulation of the detector response. Simulated signal and background events are overlaid with recorded unbiased beam crossings to incorporate the effect of multiple interactions that occur in a single beam crossing. After reconstruction, simulated events are weighted properly to ensure that the instanta-

neous luminosity distribution is the same in data and the simulated Monte Carlo (MC) samples. A parametrization of the trigger efficiency measured from the data is applied to simulated MC events in order to fold in trigger effects. The multijet background, not included in the MC samples, is directly estimated from data.

A large data sample of $Z/\gamma^*(\to ee)$ + jets events, corresponding to an integrated luminosity of 1067 ± 65 pb^{-1}, from the same data period as the $\tilde{t}$ search, is used to improve the prediction of V+jets backgrounds. For this study, Z boson candidates are selected using two high transverse energy ($E_T > 15$ GeV) clusters that deposit more than 90% of their energy in the electromagnetic calorimeter, have shower shapes consistent with expectations for electrons, are matched with tracks reconstructed in the central tracker, and form an invariant mass between 65 GeV and 115 GeV. At least two jets with $p_T > 15$ GeV and $|\eta_{\rm det}| < 2.5$ are required, where $|\eta_{\rm det}|$ is the jet pseudorapidity calculated using the assumption that the jet originates from the detector center. The predicted number of $Z/\gamma^*(\to ee)+ \geq 2$ jets events is calculated using ALPGEN after correcting for differences in electron and jet reconstruction efficiencies between data and MC and normalizing the MC to the inclusive number of Z boson events in data. The ALPGEN prediction is corrected in each jet multiplicity bin by a reweighting function that depends on the transverse momentum of the Z boson to obtain better agreement between the model and data. The reweighting function is derived by fitting the ratio of the transverse momentum distribution of Z boson data to that from the MC prediction. After reweighting, all other kinematical variables in the $Z/\gamma^*(\to ee)+ \geq 2$ jets sample applicable to the $\tilde{t}$ search are well described by MC.

The multijet background in $Z/\gamma^*(\to ee)$ + jets events is estimated from a fit to the dielectron invariant mass distribution. The ratio of the number of ee events produced by γ^* to the number of $Z+\gamma^*$ events is determined from MC and used to extract the multijet contribution by fitting the dielectron invariant mass in data with an exponential function for the multijet+γ^* contribution and a Breit-Wigner convolved with a Gaussian for Z boson events.

For the $\tilde{t}$ search, the predicted SM background from V+jets sources is normalized to the number of $Z/\gamma^*(\to ee) + 2$ jets events after subtracting the multijet background, $N_{Z(ee)+2}^{\rm data}$. As an example, the normalization weight assigned to simulated $Z(\to \nu\bar\nu)$ events with n light partons is

$$w_{\rm MC}^{Z(\nu\bar\nu)+n} = f\,\frac{N_{Z(ee)+2}^{\rm data}}{N_{Z(\nu\bar\nu)+n}^{\rm MC}}\,\frac{\sigma_{Z(\nu\bar\nu)+n}^{\rm ALP}}{\sigma_{Z(ee)+2{\rm lp}}^{\rm ALP}}\,\frac{\epsilon_{Z(\nu\bar\nu)+n}}{\epsilon_{Z(ee)+2{\rm lp}}}. \quad (1)$$

Here $N_{Z(\nu\bar\nu)+n}^{\rm MC}$ is the number of simulated $Z(\to \nu\bar\nu)+ n$ light parton jets events; $\sigma_{Z(\nu\bar\nu)+n}^{\rm ALP}$ and $\sigma_{Z(ee)+2{\rm lp}}^{\rm ALP}$ are the cross sections predicted by ALPGEN for $Z(\to \nu\bar\nu)+ n$

and $Z/\gamma^*(\to ee)+ 2$ light parton jets, respectively; and $\epsilon_{Z(\nu\bar\nu)+n}$ and $\epsilon_{Z(ee)+2{\rm lp}}$ are the corresponding detection efficiencies. The factor $f = 0.89 \pm 0.02$ is applied to correct for three effects: the absence of γ^* contribution to $Z(\nu\bar\nu)+$ jets events, the normalization of MC light jets to a data sample that contains all flavors of jets, and the difference in the luminosities of the data set used for the $\tilde{t}$ search (995 pb^{-1}) and the $Z/\gamma^*(\to ee)+2$ jets data set (1067 pb^{-1}).

The normalization weight assigned to simulated $W(\to \ell\nu)+n$ light partons is

$$w_{\rm MC}^{W(\ell\nu)+n} = f\,\frac{N_{Z(ee)+2}^{\rm data}}{N_{W(\ell\nu)+n}^{\rm MC}}\,\frac{\sigma_{W(\ell\nu)+n}^{\rm ALP}}{\sigma_{Z(ee)+2{\rm lp}}^{\rm ALP}}\,\frac{\epsilon_{W(\ell\nu)+n}}{\epsilon_{Z(ee)+2{\rm lp}}}\alpha(p_T), \quad (2)$$

where

$$\alpha(p_T) = \frac{\left[\frac{1}{\sigma_W^{\rm NLO}}\frac{d\sigma_W^{\rm NLO}}{dp_T}\right]}{\left[\frac{1}{\sigma_Z^{\rm NLO}}\frac{d\sigma_Z^{\rm NLO}}{dp_T}\right]}\frac{\left[\frac{1}{\sigma_Z^{\rm ALP}}\frac{d\sigma_Z^{\rm ALP}}{dp_T}\right]}{\left[\frac{1}{\sigma_W^{\rm ALP}}\frac{d\sigma_W^{\rm ALP}}{dp_T}\right]}, \quad (3)$$

is the product of the ratio of the normalized differential cross sections for W and Z bosons production at NLO [20] and predicted by ALPGEN, respectively.

The motivation behind using this technique is to lower the luminosity times cross section uncertainty ($\approx 6.1\% \oplus 15\%$) on the predicted number of events towards the 5% statistical uncertainty of the $Z/\gamma^*(\to ee)+2$ jets normalization sample. The combined 15% uncertainty on the theoretical cross section for various background processes is mainly due to the choice of PDF and the renormalization and factorization scale. The signal and smaller backgrounds such as $t\bar t$, diboson, and single top quark production are normalized using the measured absolute luminosity. For these processes NLO cross sections were computed with MCFM 5.1 [21].

The search strategy for $\tilde{t}$ involves three steps which include the application of the selection criteria on kinematical variables, heavy flavor (HF) tagging and optimization of the final selection depending on $\tilde{t}$ and $\tilde\chi_1^0$ masses. The data set for the $\tilde{t}$ search is reduced to a sample of 2288 potential $t\bar{\tilde{t}}$ candidates, by applying the 15 selection criteria denoted by **C1** − **C15** and summarized in Table I. The main motivation for **C1** is to reduce the multijet background. Requirements **C2** to **C7** help in reducing the W+jets and multijet backgrounds. The condition on the charged particle fraction (CPF) in **C8** requires that at least 85% of the jets' charged particle transverse momenta be associated with tracks originating from the selected primary vertex in the event. This track confirmation requirement removes events with spurious $\not{E}_T$ due to the choice of an incorrect primary vertex. **C9** − **C11** are applied to reject W+jets background with isolated leptons from W boson decay. For an electron to be isolated, the energy deposited in the calorimeter in a cone of radius 0.4 in $\eta - \phi$ around the electron direction should not be more than 15% of the energy deposited
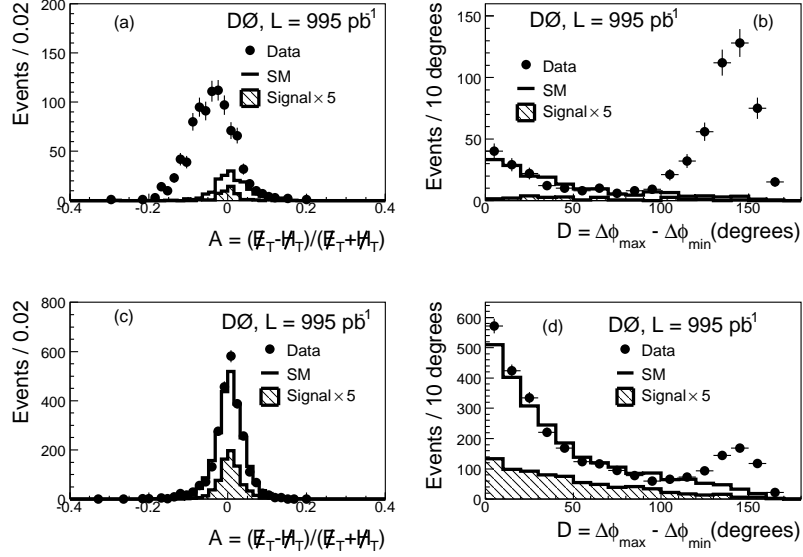
FIG. 1: Distributions of the asymmetry $A = (\not{E}_T - \not{H}_T)/(\not{E}_T + \not{H}_T)$ with the requirement on $D = \Delta\phi_{\max} - \Delta\phi_{\min}$ inverted (a) and applied (c). Distributions of D with the requirement on A inverted (b) and applied (d) for data (points with error bars), for SM backgrounds (histogram), and for a signal with $m_{\tilde{t}} = 150$ GeV and $m_{\tilde{\chi}_1^0} = 70$ GeV (hatched histogram). In all plots the signal contribution has been scaled up by five and $\not{E}_T > 60$ GeV is required. The excess in data at $A = 0$ and $D = 0 - 10$ degrees is consistent with the systematic uncertainties on the predicted background.

TABLE I: Numbers of data events and cumulative signal efficiency for $m_{\tilde{t}} = 150$ and $m_{\tilde{\chi}_1^0} = 70$ GeV after each event selection.

Selection	Events left	Signal eff. (%)
Initial selection and trigger	1.5×10^6	55.9
C1: exactly two jets	464477	29.5
C2: $\not{H}_T > 40$ GeV	440161	27.5
C3: $\Delta\phi(\text{jet}_1, \text{jet}_2) < 165°$	278505	26.5
C4: jet-1 $p_T > 40$ GeV	216382	24.7
C5: jet-1 $|\eta_{\det}| < 1.5$	113591	24.6
C6: jet-2 $p_T > 20$ GeV	80987	22.0
C7: jet-2 $|\eta_{\det}| < 1.5$	62910	20.1
C8: jet-1 jet-2 CPF > 0.85	49140	19.8
C9: isolated track veto	23832	13.4
C10: isolated electron veto	23194	13.3
C11: isolated muon veto	23081	13.3
C12: $\Delta\phi_{\max} - \Delta\phi_{\min} < 120°$	9753	12.6
C13: $A > -0.05$	3733	12.0
C14: $\Delta\phi(\text{jet}, \not{E}_T) > 50°$	3375	11.6
C15: $\not{E}_T > 60$ GeV	2288	10.0

in the electromagnetic layers inside a cone of radius 0.2. A muon is declared isolated if the sum of the energies of all tracks other than the muon in a cone of radius 0.5 is less than 2.5 GeV, and the calorimeter energy deposited in a hollow cone with inner and outer radii 0.1 and 0.4 around the muon direction is less than 5 GeV. A track with $p_T > 5$ GeV is considered isolated if no other track with $p_T > 1.5$ GeV is found in a hollow cone of inner and outer radii 0.1 and 0.4 around the track considered. This condition also helps suppress backgrounds with τ leptons where the τ decays hadronically. Remaining instrumental background is removed using a quantity defined by the angular separation between all jets and the $\not{E}_T$ of the event, $D = \Delta\phi_{\max} - \Delta\phi_{\min}$, where $\Delta\phi_{\max}$ ($\Delta\phi_{\min}$) is the largest (smallest) azimuthal separation between a jet and $\not{E}_T$; and an asymmetry variable defined as $A = (\not{E}_T - \not{H}_T)/(\not{E}_T + \not{H}_T)$. The requirements applied on these variables are given by **C12** and **C13**. Figure 1 shows that both of these variables are very effective in eliminating multijet background which dominates in data for large D and negative A.

The 2288 events selected in data can be compared to the $2199 \pm 18^{+316}_{-321}$ events predicted from the simulation normalized to $Z/\gamma^*(\to ee) + 2$ jets events or $2292 \pm 19^{+527}_{-532}$ events predicted using absolute luminosity normalization, with the first quoted uncertainty due to finite MC statistics and the second due to systematic effects described in more detail below. The small remaining multijet background in the $\tilde{t}$ search analysis is estimated after applying all analysis conditions shown in Table I except that on $\not{E}_T$. The background subtracted $\not{E}_T$ distribution is fitted in the control region ($40 \leq \not{E}_T \leq 60$ GeV) with exponential and power law functions, and the estimated contribution is extrapolated into the signal region ($\not{E}_T > 60$ GeV). The average of the two results is taken as the multijet background estimate, while the difference between the two fit results is taken as the systematic
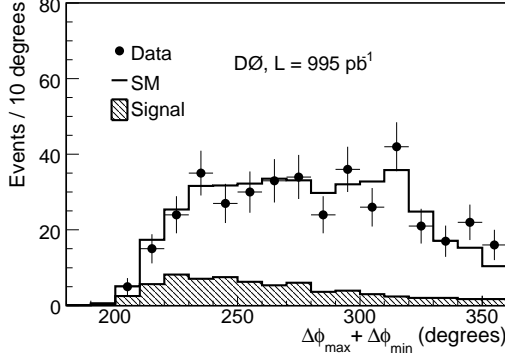
FIG. 2: Distributions of $S = \Delta\phi_{\max} + \Delta\phi_{\min}$ for data (points with error bars), SM background (histogram), and a signal with $m_{\tilde{t}} = 150$ GeV and $m_{\tilde{\chi}_1^0} = 70$ GeV (hatched histogram) after requiring HF tagging but before optimization.

TABLE II: Optimized values of selections, numbers of observed data and predicted background events. A requirement of $\not{E}_T > 70$ GeV was chosen in all cases. The values of $m_{\tilde{t}}$ and H_T are in GeV while those for S are in degrees.

$m_{\tilde{t}}$	H_T	S	Observed	Predicted
$95 - 130$	> 100	< 260	83	$85.3 \pm 1.8^{+12.8}_{-13.0}$
$135 - 145$	> 140	< 300	57	$59.0 \pm 1.6^{+8.5}_{-8.8}$
$150 - 160$	> 140	< 320	66	$66.6 \pm 1.1^{+9.6}_{-10.0}$

TABLE III: For three $\tilde{t}$ and $\tilde{\chi}_1^0$ mass combinations: signal efficiencies and the numbers of signal events expected. The first errors are statistical and second systematic. The nominal (NLO) signal cross section and upper limit at the 95% C.L. are also shown.

$(m_{\tilde{t}}, m_{\tilde{\chi}_1^0})$	Efficiency	Expected Signal	σ_{nom}	σ_{95}
GeV	(%)	Events	pb	pb
$(130, 55)$	1.5	$51.9 \pm 2.7^{+7.2}_{-7.1}$	3.44	2.41
$(140, 80)$	0.9	$19.6 \pm 0.8^{+2.8}_{-2.5}$	2.24	2.87
$(150, 70)$	2.1	$30.8 \pm 1.2^{+4.2}_{-3.7}$	1.49	1.42

uncertainty. This amounts to 14.4 ± 10.7 (stat) ± 5.1 (sys) events contributed by multijet background before HF tagging and optimization of selection cuts.

After selecting candidate events on the basis of topology, HF tagging is used to identify charm jets in the final state. A neural network (NN) tagging tool [22] that combines information from three different D0 HF taggers to maximize the b quark tagging efficiency ($\approx 73\%$) is used for this purpose.

The first tagger converts information from the impact parameter of the tracks identified in a jet into a probability that all tracks originate from the primary vertex, where the impact parameter is the distance of closest approach to the interaction point in a plane perpendicular to the beam axis. The second tagger identifies the presence of vertices that are significantly displaced from the primary vertex and associated with a jet. The third tagger makes use of the number of tracks with large impact parameter significance, where the significance is defined as the ratio of the impact parameter to its uncertainty. The result of the combination is a NN output. A requirement on the NN output is made that preserves high efficiency for detection of charm jets ($\approx 30\%$) with a $\approx 6\%$ probability for a light parton jet to be mistakenly tagged. The efficiency for c jet tagging is obtained by scaling the b jet tagging efficiency measured in the data by the c-tagging-to-b-tagging efficiency ratio computed in the MC.

At the final stage of the analysis, additional selection criteria on three kinematic variables; $\not{E}_T$, $S = \Delta\phi_{\max} + \Delta\phi_{\min}$, and H_T, with H_T defined as the scalar sum of the p_T of all jets, are optimized by maximizing the expected lower limit on the neutralino mass for a given $m_{\tilde{t}}$. The variable S after requiring at least one jet in the event to be HF tagged is shown in Fig. 2.

Minimum values of H_T are varied from 60 GeV to 140 GeV in steps of 20 GeV, while those for $\not{E}_T$ are var-

ied from 60 GeV to 100 GeV in steps of 10 GeV. Events having the values of these quantities above the minima are kept. Maximum values of S are tested between 240° and 320° in steps of 20°, and events having S below the minimum are retained. For each set of requirements, the expected value of the signal confidence level $\langle CL_s \rangle$ [23] under the hypothesis that only background is present is evaluated using all $\tilde{t}$ and $\tilde{\chi}_1^0$ mass combinations, taking into account systematic uncertainties. The set of criteria that return $\langle CL_s \rangle = 0.05$ for the highest neutralino mass corresponding to a given $m_{\tilde{t}}$ are chosen to be the optimal ones.

The optimized values of the selections for different $m_{\tilde{t}}$ are given in Table II along with the number of events observed in data and expected SM background. In all cases a requirement of $\not{E}_T \geq 70$ GeV is imposed. No contamination remains from multijet background at this point in the analysis; it is therefore neglected while setting the limit. Efficiencies for three signal mass points along with the expected numbers of events are shown in Table III. The distribution of H_T after optimization but with the constraint on H_T removed is shown in Fig. 3. The final distribution of $\not{E}_T$ is shown in Fig. 4. The detailed SM
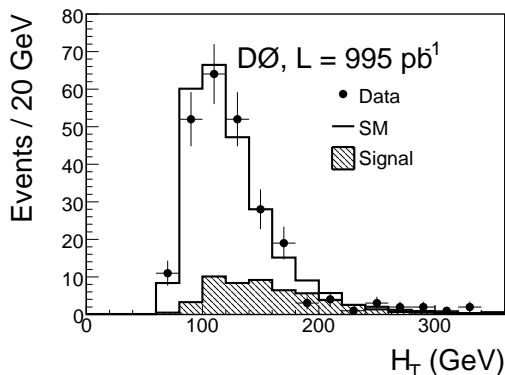
FIG. 3: Distributions of H_T after applying optimized requirements on $\not{E}_T$ and S for data (points with error bars), SM background (histogram), and a signal with $m_{\tilde{t}} = 150$ GeV and $m_{\tilde{\chi}_1^0} = 70$ GeV (hatched histogram).
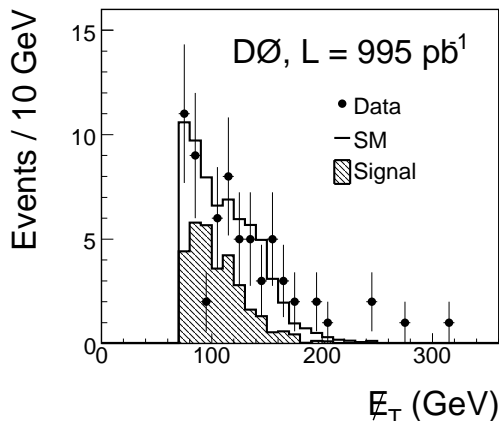

FIG. 4: Final distributions of $\not{E}_T$ for data (points with error bars), SM background (histogram), and a signal with $m_{\tilde{t}} = 150$ GeV and $m_{\tilde{\chi}_1^0} = 70$ GeV (hatched histogram).

background composition is given in Table IV.

Systematic uncertainties are evaluated for each $\tilde{t}$ and $\tilde{\chi}_1^0$ mass combination for the optimized set of requirements. Sources of systematic uncertainty include jet energy scale, jet energy resolution, jet identification and reconstruction, the jet multiplicity requirement, trigger efficiency, data to MC scale factors, normalization of background, HF tagging, luminosity determination, choice of PDF, and W boson p_T reweighting. The effect of the jet multiplicity requirement on the background is studied using $Z/\gamma^*(\to ee)$ + jets events. The spectrum of transverse momentum of the third jet in data events with three or more jets is observed to be very well described by the simulation generated with ALPGEN. The $\approx 1\%$ statistical uncertainty of the lowest p_T bin, where the bulk of the events are, is taken as a systematic uncertainty introduced by the jet multiplicity requirement. To study the effect of the same requirement on the $\tilde{t}$ signal, where

TABLE IV: Numbers of predicted background events from different SM sources for a selection optimized for $m_{\tilde{t}} \geq 150$ GeV. The uncertainties are due to the limited MC statistics.

SM process	Number of events
$W(\to \ell\nu)$ + jets	20.0 ± 0.7
$Z(\to \nu\bar{\nu})$ + jets	15.8 ± 0.5
$W(\to \ell\nu)$ + HF ($b\bar{b}, c\bar{c}$)	12.6 ± 0.5
$Z(\to \nu\bar{\nu})$ + HF ($b\bar{b}, c\bar{c}$)	11.6 ± 0.4
$t\bar{t}$ and single top	3.7 ± 0.1
WW, WZ, ZZ	2.7 ± 0.1
$Z(\to \ell\ell)$ (e, μ, τ) + jets	0.1 ± 0.01
$Z(\to \ell\ell)$ (e, μ, τ) + HF ($b\bar{b}, c\bar{c}$)	0.1 ± 0.01
Total	66.6 ± 1.1

a third jet enters an event primarily through initial or final state radiation, the p_T spectrum of the leading jet in simulated $Z/\gamma^*(\to ee)$ events generated with PYTHIA is examined. Comparison between data and simulation shows a slight excess in data in the low p_T bin; this discrepancy is used to estimate a systematic uncertainty of $\pm 1.5\%$ on the signal acceptance attributable to the jet multiplicity requirement. The uncertainty on the signal acceptance and background estimation due to the PDF choice was determined using the CTEQ6.1M PDF set.

The combined 10% uncertainty on the background normalization includes: 5% uncertainty from $Z/\gamma^*(\to ee)$ + jets statistics assigned to all V+jets samples; 50% uncertainty on the NLO cross section assigned to the V + HF background; 6.1% luminosity uncertainty assigned to $t\bar{t}$, diboson, single top quark background; and $8\%, 6\%$ and 15% uncertainties on NLO cross sections for $t\bar{t}$, diboson, and single top quark production, respectively. The uncertainty on the background estimation due to the W boson p_T reweighting is estimated using two different methods to estimate the W+jets background. In the first method, the W+jets background is estimated using the expression given in Eq. 2. In the second method, the same reweighting function as applied to the Z boson was used to reweight the W boson p_T which is equivalent to setting $\alpha(p_T) = 1$ in Eq. 2. Detailed estimates of all systematic uncertainties are given in Table V.

Using the assumption that $\tilde{t}$ decays into a charm quark and a neutralino with 100% branching fraction and the nominal $\tilde{t}$ pair production cross section, the largest $m_{\tilde{t}}$ excluded by this analysis is 155 GeV, for a neutralino mass of 70 GeV at the 95% C.L. With the theoretical uncertainty on the $\tilde{t}$ pair production cross section taken into account, the largest limit on $m_{\tilde{t}}$ is 150 GeV, for $m_{\tilde{\chi}_1^0} = 65$ GeV. These results are shown in Fig. 5.

In summary, D0 has searched for scalar top quarks in jets plus missing transverse energy final states using 1 fb^{-1} of data. No evidence for $\tilde{t}$ production has been found. This analysis substantially extends the excluded

TABLE V: Breakdown of systematic uncertainties on the SM background and for a signal point with $m_{\tilde{t}} = 150$ GeV and $m_{\tilde{\chi}_1^0} = 70$ GeV.

Source	SM background	Signal
Jet energy	+1.7%	+2%
scale	−2.5%	−4%
Jet resolution	±1%	±1%
Jet reconstruction and identification	±0.8%	±0.1%
Trigger	±6%	±6%
Scale factor	±5%	±5%
Normalization	±10%	−
Luminosity	−	±6.1%
HF tagging	±4.1%	±3.5%
PDF choice	±4%	+8.7%
	−	−5.5%
Two jet cut	±0.9%	±1.5%
W boson p_T reweighting	±3%	−
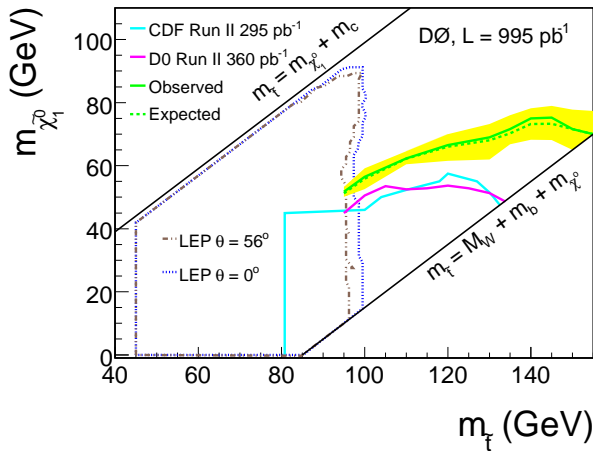
FIG. 5: Region in the $\tilde{t}$–$\tilde{\chi}_1^0$ mass plane excluded at the 95% C.L. by the present search. The observed (expected) exclusion contour is shown as the green solid (dashed) line. The yellow band represents the theoretical uncertainty on the scalar top quark pair production cross section due to PDF and renormalization and factorization scale choice. Results from previous searches [8, 10, 12] are also shown.

region of the $\tilde{t} - \tilde{\chi}_1^0$ mass plane over the searches carried out previously.

[a] Visitor from Augustana College, Sioux Falls, SD, USA.
[b] Visitor from The University of Liverpool, Liverpool, UK.
[c] Visitor from ICN-UNAM, Mexico City, Mexico.
[d] Visitor from II. Physikalisches Institut, Georg-August-University, Göttingen, Germany.
[e] Visitor from Helsinki Institute of Physics, Helsinki, Finland.
[f] Visitor from Universität Zürich, Zürich, Switzerland.
[‡] Deceased.
[1] H. Baer et al., Phys. Rev. D 50, 4517 (1994) and references therein.
[2] D. Delepine et al., Phys. Lett. B 386, 183 (1996).
[3] P. Fayet, Phys. Lett. B 238, 489 (1977).
[4] J. Ellis et al., Nucl. Phys. B238 453 (1984).
[5] C. Boehm, A. Djouadi, Y. Mambrini, Phys. Rev. D 61, 095006 (2000).
[6] W. Beenakker et al., Nucl. Phys. B515 3 (1998).
[7] J. Pumplin et al., JHEP 0207, 012 (2002) and D. Stump et al., JHEP 0310, 046 (2003).
[8] LEPSUSYWG Collaboration, ALEPH Collaboration, DELPHI Collaboration, L3 Collaboration, OPAL Collaboration, Note LEPSUSYWG/04-02.1, http://lepsusy.web.cern.ch/lepsusy/www/squarks_summer04/sto
[9] T. Affolder et al. (CDF Collaboration), Phys. Rev. Lett. 84, 5704 (2000).
[10] T. Aaltonen et al. (CDF Collaboration), Phys. Rev. D 76, 072010 (2007).
[11] V.M. Abazov et al. (D0 Collaboration), Phys. Rev. Lett. 93, 011801 (2004).
[12] V.M. Abazov et al. (D0 Collaboration,) Phys. Lett. B 645, 119 (2007).
[13] T. Andeen et al., FERMILAB-TM-2365 (2007).
[14] V.M. Abazov et al. (D0 Collaboration), Nucl. Instrum. Methods Phys. Res. A 565, 463 (2006).
[15] G.C. Blazey et al., in Proceedings of the Workshop: QCD and Weak Boson Physics in Run II, edited by U. Baur, R.K. Ellis, and D. Zeppenfeld, Fermilab-Pub-00/297 (2000).
[16] T. Sjöstrand et al., Comput. Phys. Commun. 135, 238 (2001).
[17] M.L. Mangano et al., JHEP 0307, 001 (2003).
[18] E. Boos et al. (CompHEP Collaboration), Nucl. Instrum. Methods Phys. Res. A 534, 250 (2004).
[19] R. Brun and F. Carminati, CERN Program Library Long Writeup W5013, 1993 (unpublished).
[20] K. Melnikov and F. Petriello, Phys. Rev. D 74, 114017 (2006).
[21] J.M. Campbell and R.K. Ellis, Phys. Rev. D 60, 113006 (1999).
[22] T. Scanlon, Ph.D. thesis, Imperial College London, FERMILAB-THESIS-2006-43, 2006.
[23] T. Junk, Nucl. Instrum. Methods Phys. Res. A 434, 435 (1999); A. Read, in "1st Workshop on Confidence Lim-

its," CERN Report No. CERN-2000-005, 2000.